
p -MLMC for acoustic scattering from large deviation rough random surfaces

Jürgen Dölz, Wei Huang, **Michael Multerer**

Università della Svizzera italiana



Outline

- 1. Problem formulation**
- 2. Simulation of random shape deformations**
- 3. Quantities of interest**
- 4. Numerical results**



Problem formulation

- Consider an incident plane wave $u_{\text{inc}}(\mathbf{x}) = e^{i\kappa \langle \mathbf{d}, \mathbf{x} \rangle}$ with known wavenumber κ and direction $\mathbf{d} \in \mathbb{R}^3$.
- If this wave is scattered at a random scatterer $D(\omega)$ the total wave

$$u(\omega) = u_{\text{inc}} + u_s(\omega)$$

is a random field.

- It is obtained by solving the exterior boundary value problem

$$\Delta u(\omega) + \kappa^2 u(\omega) = 0 \quad \text{in } \mathbb{R}^3 \setminus \overline{D(\omega)},$$

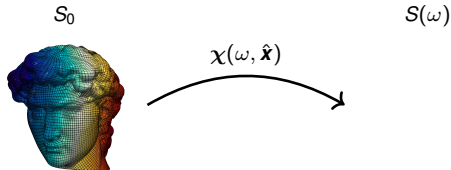
$$u(\omega) = 0 \quad \text{at } S(\omega) := \partial D(\omega),$$

$$\sqrt{r} \left(\frac{\partial u_s(\omega)}{\partial r} - i\kappa u_s(\omega) \right) \rightarrow 0 \quad \text{as } r := \|\mathbf{x}\|_2 \rightarrow \infty.$$

- We employ the (isogeometric) boundary element method for the solution.



Representation of random shapes



- We represent $S(\omega)$ by a random deformation field.
- More precisely, we assume that there is a uniform C^1 -diffeomorphism $\chi: \Omega \times S_0 \rightarrow \mathbb{R}^3$, i.e.

$$\|\chi(\omega)\|_{C^1(S_0; \mathbb{R}^3)}, \|\chi^{-1}(\omega)\|_{C^1(S(\omega); \mathbb{R}^3)} \leq C_{\text{uni}} \quad \text{for } \mathbb{P}\text{-a.e. } \omega \in \Omega$$

such that

$$S(\omega) = \chi(\omega, S_0) \quad \text{for } \mathbb{P}\text{-a.e. } \omega \in \Omega.$$



Karhunen-Loève expansion

- Similarly to scalar fields, we model them by their *expected value*

$$\mathbb{E}[\chi](\mathbf{x}) := \int_{\Omega} \chi(\omega, \mathbf{x}) d\mathbb{P} = \mathbf{x}, \quad \mathbb{E}[\chi]: S_0 \rightarrow \mathbb{R}^d$$

and their *covariance function* $\text{Cov}[\chi]: S_0 \times S_0 \rightarrow \mathbb{R}^{d \times d}$

$$\text{Cov}[\chi](\mathbf{x}, \mathbf{x}') := \int_{\Omega} \chi_0(\omega, \mathbf{x}) \chi_0^\top(\omega, \mathbf{x}') d\mathbb{P}, \quad \text{where } \chi_0 := \chi - \mathbb{E}[\chi].$$

- Then, the *Karhunen-Loève expansion* of $\chi(\omega, \mathbf{x})$ is given by

$$\chi(\omega, \mathbf{x}) = \mathbf{x} + \sum_{k=1}^{\infty} \sqrt{\lambda_k} Y_k(\omega) \chi_k(\mathbf{x}),$$

where $\{(\lambda_k, \chi_k)\}_k$ are the eigen pairs of the covariance operator and $\{Y_k\}_k$ are uncorrelated random variables with $\mathbb{V}[Y_k] = 1$.

- For computations, the Karhunen-Loève expansion is truncated after m terms.



Geometry representation

- We adopt the usual isogeometric setting for the representation of S_0 , i.e.

$$S_0 = \bigcup_{i=1}^M S_0^{(i)},$$

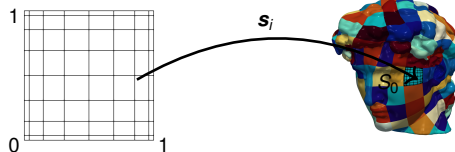
- Each patch $S_0^{(i)}$ is represented by a smooth, invertible (NURBS) mapping

$$\mathbf{s}_i: [0, 1]^2 \rightarrow S_0^{(i)} \quad \text{with} \quad S_0^{(i)} = \mathbf{s}_i([0, 1]^2) \quad \text{for } i = 1, 2, \dots, M.$$

- The intersection $S_0^{(i)} \cap S_0^{(i')}$ consists at most of a common vertex or a common edge for $i \neq i'$.
- To obtain realizations of $S(\omega)$, we consider the mappings $\chi(\omega) \circ \mathbf{s}_i$, for $i = 1, \dots, M$.



Geometry reinterpolation



- Given a polynomial degree q , we introduce the grid of tensor product of Chebyshev points of the second kind, i.e.,

$$\xi_{\ell,\ell'} := [\xi_\ell \ \xi_{\ell'}]^T, \quad \ell, \ell' = 0, \dots, q$$

on the unit square \square .

- Interpolating s_i by tensor product Lagrange polynomials, we arrive at

$$s_i(s, t) \approx \sum_{\ell=0}^q \sum_{\ell'=0}^q s_i(\xi_{\ell,\ell'}) L_\ell(s) L_{\ell'}(t).$$



Barycentric interpolation of random deformation fields

- The mapped points

$$\mathbf{p}_{i,\ell,\ell'} := \mathbf{s}_i(\xi_{\ell,\ell'}), \quad \theta := \{\mathbf{p}_{i,\ell,\ell'} : i = 1, \dots, M, \ell, \ell' = 0, \dots, q\}$$

serve as landmark points for the representation of the random surface.

- The deformation field is now represented patchwise according to

$$\chi(\omega, \mathbf{s}_i(s, t)) \approx \sum_{\ell=0}^q \sum_{\ell'=0}^q \chi(\omega, \mathbf{p}_{i,\ell,\ell'}) L_\ell(s) L_{\ell'}(t).$$

- The stable evaluation is achieved by the barycentric interpolation formula

$$\chi(\omega, \mathbf{s}_i(s, t)) \approx \rho(s)\rho(t) \sum_{\ell,\ell'=0}^q \frac{w_\ell}{s - \xi_\ell} \frac{w'_{\ell'}}{t - \xi_{\ell'}} \chi(\omega, \mathbf{p}_{i,\ell,\ell'}),$$

where

$$\rho(s) := \left(\sum_{\ell=0}^q \frac{w_\ell}{s - \xi_\ell} \right)^{-1} \quad \text{and} \quad w_\ell := \prod_{j \neq \ell} \frac{1}{\xi_\ell - \xi_j}.$$



Simulation of random deformation fields

- To evaluate the Karhunen-Loëve expansion at the landmark points, we solve the eigenvalue problem for the covariance matrix

$$\mathbf{C} := [\text{Cov}[\chi](\mathbf{p}_{i,k,k'}, \mathbf{p}_{j,\ell,\ell'})] \in \mathbb{R}^{3n \times 3n}, \quad n := |\theta| = M(q+1)^2.$$

- Solving the eigenvalue problem naively is of cost $\mathcal{O}(27n^3)$. Instead, we use a low-rank approach via the pivoted Cholesky decomposition.
- Given $\mathbf{C} \approx \mathbf{L}\mathbf{L}^\top$, rank $\mathbf{L} = m \ll 3n$, we solve $\mathbf{L}\mathbf{L}^\top \mathbf{v} = \lambda \mathbf{v}$ via $\mathbf{L}^\top \mathbf{L} = \tilde{\mathbf{V}} \Lambda \tilde{\mathbf{V}}^\top$.
- If $(\lambda, \tilde{\mathbf{v}}_i)$ is an eigenpair of the latter, $(\lambda_k, \mathbf{L}\tilde{\mathbf{v}}_k)$ is an eigenpair of the former.
- It holds

$$\chi(\mathbf{y}, \theta) \approx \theta + \text{reshape}(\mathbf{L}\tilde{\mathbf{V}}\mathbf{y}, n, 3),$$

where $\mathbf{y} = [Y_1(\omega), \dots, Y_m(\omega)]^\top \in \mathbb{R}^m$.



Boundary integral formulation

- The Neumann data of the total wave $u = u_{\text{inc}} + u_s$ at the surface S can be determined by the Kress formulation

$$\left(\frac{1}{2} + \mathcal{K}^* - i\eta \mathcal{V} \right) \frac{\partial u}{\partial \mathbf{n}} = \frac{\partial u_{\text{inc}}}{\partial \mathbf{n}} - i\eta u_{\text{inc}} \quad \text{at } S,$$

with $\eta = \kappa/2$.

- From the Cauchy data of u at S , we can determine the scattered wave u_s at any exterior point by applying the potential evaluation

$$u_s(\mathbf{x}) = \int_S \Phi(\mathbf{x}, \mathbf{z}) \frac{\partial u}{\partial \mathbf{n}_z}(\mathbf{z}) d\sigma_z, \quad \Phi(\mathbf{x}, \mathbf{z}) := \frac{e^{i\kappa \|\mathbf{x}-\mathbf{z}\|_2}}{4\pi \|\mathbf{x}-\mathbf{z}\|_2}, \quad \mathbf{x} \in \mathbb{R}^3 \setminus \bar{D}.$$



Quantities of interest

- For any locations \mathbf{x} and \mathbf{x}' outside the obstacle, we obtain by (bi)linearity

$$\mathbb{E}[u_s](\mathbf{x}) := \mathbb{E} \left[\int_{S(\omega)} \Phi(\mathbf{x}, \mathbf{z}) \frac{\partial u}{\partial \mathbf{n}_z}(\mathbf{z}, \cdot) d\sigma_z \right]$$

$$\text{Cor}[u_s](\mathbf{x}, \mathbf{x}') := \mathbb{E} [u_s(\mathbf{x}, \omega) \overline{u_s}(\mathbf{x}', \omega)].$$

- Obviously, this formulation is not very practical, if we are interested in evaluating the QoI's at many locations.
- Resort: We introduce an artificial interface T that almost surely contains the realisations of the scatterer.



Quantities of interest II

- Using the artificial interface T , we have the representation formula

$$u_s(\mathbf{x}) = \int_T \Phi(\mathbf{x}, \mathbf{z}) \frac{\partial u_s}{\partial \mathbf{n}_z}(\mathbf{z}) - \frac{\partial \Phi(\mathbf{x}, \mathbf{z})}{\partial \mathbf{n}_z} u_s(\mathbf{z}) d\sigma_{\mathbf{z}}.$$

- Now, exploiting (bi)linearity of the expectation yields

$$\mathbb{E}[u_s](\mathbf{x}) = \int_T \left\{ \Phi(\mathbf{x}, \mathbf{z}) \mathbb{E}\left[\frac{\partial u_s}{\partial \mathbf{n}_z} \right](\mathbf{z}) - \frac{\partial \Phi(\mathbf{x}, \mathbf{z})}{\partial \mathbf{n}_z} \mathbb{E}[u_s](\mathbf{z}) \right\} d\sigma_{\mathbf{z}},$$

$$\begin{aligned} & \text{Cor}[u_s](\mathbf{x}, \mathbf{x}') \\ &= \int_T \int_T \left\{ \Phi(\mathbf{x}, \mathbf{z}) \overline{\Phi(\mathbf{x}', \mathbf{z}')} \text{Cor}\left[\frac{\partial u_s}{\partial \mathbf{n}} \right](\mathbf{z}, \mathbf{z}') - \Phi(\mathbf{x}, \mathbf{z}) \overline{\frac{\partial \Phi(\mathbf{x}', \mathbf{z}')}{\partial \mathbf{n}_{\mathbf{z}'}}} \text{Cor}\left[\frac{\partial u_s}{\partial \mathbf{n}} \right](\mathbf{z}, \mathbf{z}') \right. \\ &\quad \left. - \frac{\partial \Phi(\mathbf{x}, \mathbf{z})}{\partial \mathbf{n}_z} \overline{\Phi(\mathbf{x}', \mathbf{z}')} \text{Cor}\left[u_s, \frac{\partial u_s}{\partial \mathbf{n}} \right](\mathbf{z}, \mathbf{z}') + \frac{\partial \Phi(\mathbf{x}, \mathbf{z})}{\partial \mathbf{n}_z} \overline{\frac{\partial \Phi(\mathbf{x}', \mathbf{z}')}{\partial \mathbf{n}_{\mathbf{z}'}}} \text{Cor}[u_s](\mathbf{z}, \mathbf{z}') \right\} d\sigma_{\mathbf{z}'} d\sigma_{\mathbf{z}}. \end{aligned}$$



p -multilevel Monte Carlo

- The formulation with the artificial interface is perfectly suited for p -multilevel quadrature approaches.
- For the expectation, we employ the approximation

$$\mathbb{E}[\rho](\mathbf{z}) \approx \sum_{p=0}^P \mathcal{Q}_{P-p}(\rho^{(p)}(\cdot, \mathbf{z}) - \rho^{(p-1)}(\cdot, \mathbf{z})).$$

- Correlation terms are approximated by

$$\text{Cor}[\rho \otimes \mu](\mathbf{z}, \mathbf{z}') \approx \sum_{p=0}^P \mathcal{Q}_{P-p}((\rho \otimes \mu)^{(p)}(\cdot, \mathbf{z}, \mathbf{z}') - (\rho \otimes \mu)^{(p-1)}(\cdot, \mathbf{z}, \mathbf{z}')).$$



Why p -refinement?

| | $p/j = 1$ | $p/j = 2$ | $p/j = 3$ | $p/j = 4$ | $p/j = 5$ | $p/j = 6$ |
|-----------------|-----------|-----------|-----------|-----------|-----------|-----------|
| h -refinement | 26 | 98 | 386 | 1538 | 6146 | 24578 |
| p -refinement | 8 | 26 | 56 | 98 | 152 | 218 |

- Comparison of the degrees of freedom issuing from h -refinement and p -refinement on the unit sphere with 6 patches.
- For the h -refinement, we consider piecewise linear ansatz functions.
- In case of p -refinement, the linear systems remain very small and suggest the use of direct solvers.



Implementation



Boundary Element Method Based Engineering Library
www.bembel.eu

[Dölz, Harbrecht, Kurz, Multerer, Schöps, Wolf, 20]

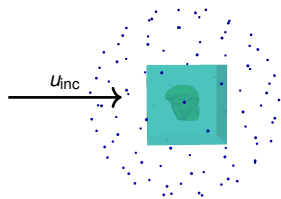
3D Laplace, Helmholtz, and Maxwell BEM Code in C++

Isogeometric and parametric surfaces
Higher-order and isogeometric boundary elements
 \mathcal{H}^2 -compression
OpenMP-Parallelization
Header-only



Experimental setup

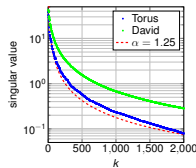
- We consider a torus and Michelangelo's Davide as D_0 , respectively.
- The artificial interface T is given by the cuboid $[-2, 2] \times [-2, 2] \times [-2, 2]$.
- For evaluation, 100 points on a sphere are used.
- We consider an incident plane wave with wavenumber $\kappa = 5$ and direction $\mathbf{d} = (1, 0, 0)$.
- The deformation field is given by $\mathbb{E}[\chi](\hat{\mathbf{x}}) = \hat{\mathbf{x}}$ and



$$\text{Cov}[\chi](\hat{\mathbf{x}}, \hat{\mathbf{x}'}) = \begin{bmatrix} k_{\frac{3}{2}}(20r) & 10^{-4}k_{\infty}(4r) & 10^{-4}k_{\infty}(4r) \\ 10^{-4}k_{\infty}(4r) & k_{\frac{3}{2}}(20r) & 10^{-4}k_{\infty}(4r) \\ 10^{-4}k_{\infty}(4r) & 10^{-4}k_{\infty}(4r) & k_{\frac{3}{2}}(20r) \end{bmatrix}.$$

Experimental setup II

- The singular values in the Karhunen-Loève expansion decay like $\sigma_k \sim k^{-1.25}$. This leads to $m = 2218, 5563$ ($\varepsilon = 10^{-3}$) for the torus and Davide, respectively.



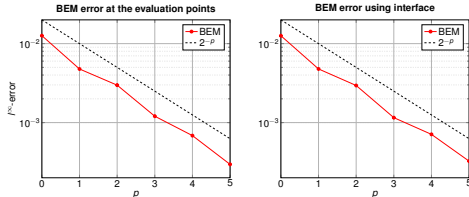
- The number of samples for the maximal degree P is fixed to 128. With increasing level, we decrease the number of samples by a factor of

$$\hat{\gamma}_p = \sqrt{\frac{\hat{v}_{p-1}}{\hat{v}_p}} \sqrt{\frac{\hat{c}_p}{\hat{c}_{p-1}}}.$$

- The p -multilevel Monte Carlo solution with degree $P + 1$ as reference.



Convergence of the boundary element method

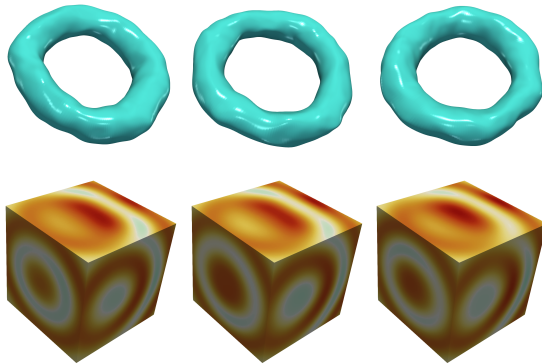


- Convergence with and without using the artificial interface for Davide.

| | $p = 0$ | $p = 1$ | $p = 2$ | $p = 3$ | $p = 4$ | $p = 5$ |
|------|---------|---------|---------|---------|---------|---------|
| t | 1.308s | 1.351s | 3.56s | 11.87s | 33.9s | 101.8s |
| DOFs | 748 | 1683 | 2992 | 4675 | 6732 | 9163 |

- Runtimes of a single run using 20 threads on a compute node with 2 x AMD 7742 CPU@2.2 GHz. Sampling is performed using 64 MPI ranks.

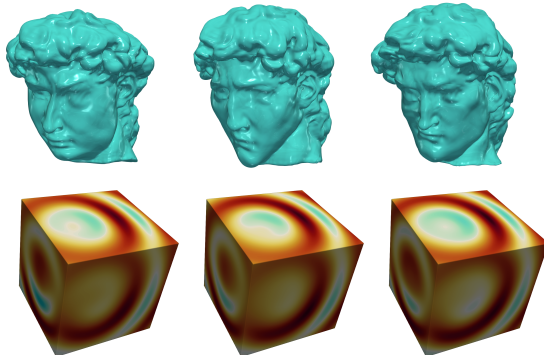
Realizations of the scattered wave



- Realizations of the scatterer and the scattered wave at the interface.



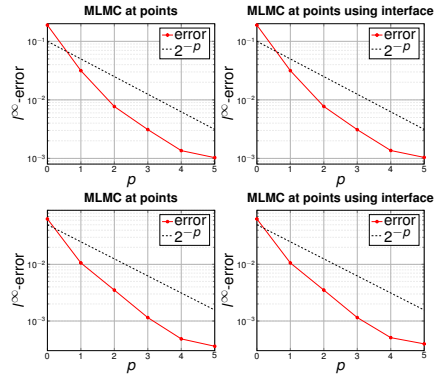
Realizations of the scattered wave



- Realizations of the scatterer and the scattered wave at the interface.



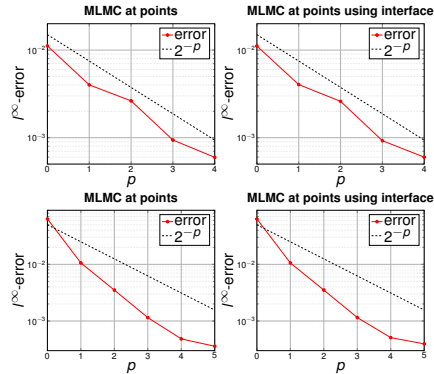
Convergence of expectation and correlation for the torus



■ Convergence of the expectation and correlation towards the reference.



Convergence of expectation and correlation for Davide



■ Convergence of the expectation and correlation towards the reference.



Conclusion

- We have solved the acoustic random scattering problem by means of an isogeometric boundary element method.
- Realizations of the random scatterer can efficiently be obtained from barycentric interpolation at landmark points.
- Using p -refinement for the boundary element method enables the use of the p -multilevel Monte Carlo method.



Thank you

References

J.-P. Berrut and L.N. Trefethen.

Barycentric Lagrange interpolation. SIAM Rev., 2004.

J. Dölz, H. Harbrecht, S. Kurz, M.D. Multerer, S. Schöps, and F. Wolf.

Bembel: The fast isogeometric boundary element C++ library for Laplace, Helmholtz, and electric wave equation. SoftwareX, 2020.

J. Dölz, H. Harbrecht, C. Jerez-Hanckes, and M. Multerer.

Isogeometric multilevel quadrature for forward and inverse random acoustic scattering. Comput. Methods Appl. Mech. Engrg., 2022.

J. Dölz, W. Huang, and M. Multerer.

p -multilevel Monte Carlo for acoustic scattering from large deviation rough random surfaces, arXiv:2311.12565, 2023.

M.B. Giles.

Multilevel monte carlo methods. Acta Numerica, 2015.

M.D. Multerer

A note on the domain mapping method with rough diffusion coefficients, Appl. Numer. Math., 2019.

